Computational Materials Science 94 (2014) 279–284

Contents lists available at ScienceDirect

Computational Materials Science

journal homepage: www.elsevier.com/locate/commatsci

Description of deformations in the elastic strain engineering of nanostructure

Ryszard Pyrz *

Department of Mechanical and Manufacturing Engineering, Aalborg University, Fibigerstræde 16, 9220 Aalborg East, Denmark

ARTICLE INFO

Article history:
Received 21 December 2013
Received in revised form 9 May 2014
Accepted 26 May 2014
Available online 26 June 2014

Keywords:
Nanostructures
Deformation gradient
Functional properties
Non-homogeneous deformation
Inhomogeneity measure

ABSTRACT

In the present investigation we elaborate on the development of a second-order elastic deformation gradient in discrete/atomistic system. Whereas deformation kinematics is typically characterized by the Cauchy–Born rule that enforces homogeneous deformation, the second-order deformation gradient allows capturing highly non-homogeneous deformations. This is particularly important in nanosystems with strain engineered functionalities. The local inhomogeneity measure has been derived from the deformation mapping to determine variability of the deformation field of nanostructures under loading. It is shown that the knowledge about the non-homogeneous deformation pattern is necessary to provide a quantitative connection to functional properties of nanostructures.

1. Introduction

Several investigations have studied the influence of mechanical strain on the functional characteristics of nanostructures and nanodevices. The idea of elastic strain engineering [1] has recently gained a considerable attention and a substantial number of investigations have been reported for different nanostructures. In carbon nanotubes application of elastic strain allows controlling electrical conductance [2], tuning the band gap changes [3–5], alter chemical reactivity [6] and in combination with simultaneously applied electric field induce changes in their electrostatic characteristics [7,8]. In silicon nanowires the compressive elastic strain dramatically decreases deformation potentials which may result in a strong increase in electron mobility [9]. Strain components have a dramatic influence on electronic states of silicon nanocrystal quantum dots [10], photoluminescence of silicon nanoclusters [11], visible and near-IR emission from single crystal silicon nanopillars [12], energy bands and band gaps in single walled silicon nanotubes [13] and optical properties of silicon optoelectronic devices [14]. Electronic-mechanical coupling has been investigated in graphene [15–17], graphene nanobubbles [18] and graphene/BN bilayers [19]. Other investigated nanosystems comprise InAs/GaAs quantum dots [20,21], boron nitride nanoribbons [22] and SiGe wells [23].

The atomistic simulations have been developed not only to provide necessary physical and/or chemical characteristics but also to create a basis for attempting to bridge the gap between atomistic systems and the continuum. However, the discrete atomistic nature of nanostructures necessitates reformulation of stress and strain concepts applicable in the continuum framework which breaks down at certain length scales [24–27]. Although different strain measures can be formulated all of them rely on the position of atoms and their displacement under deformation of the atomic system. The position of atoms is usually accessed from coordinates of atoms that follow from atomistic simulations. In specific circumstances it is also possible to determine atomic positions and corresponding displacement field from high resolution images [28–34]. Gullet et al. [35] have shown that the small strain approximation frequently utilized in continuum mechanics should not be used to describe atomic strains particularly for non-homogeneous deformations. They derive atomic strain model which is based on the discretized deformation gradients which correspond to the finite strain measure in continuum settings. Furthermore, the classical Cauchy–Born rule that relates affine displacement boundary conditions to affine homogeneous deformations is generally not valid at atomic scale [36–39] and developments of the second order-deformation gradients are necessary to capture nonhomogeneous deformations [40–43].

In the present work, the deformation measures that are based on the definition of a discrete equivalent to the continuum second-order deformation gradient are derived to capture non-homogeneous deformations of the atomistic system. It is demonstrated

* Tel.: +45 9940 9326; fax: +45 9940 7110.
E-mail address: rp@m-tech.aau.dk

http://dx.doi.org/10.1016/j.commatsci.2014.05.057
0927-0256/

that the introduction of the second-order deformation gradient allows correct description of atomic positions in a deformed state under highly non-homogeneous deformations. Furthermore, non-homogeneity descriptors are introduced to relate degree of non-affinity to functional properties of the atomic system.

2. Calculation procedures

2.1. Quantum-mechanical simulations

Atomistic calculations have been performed with the self-consistent field (SCF) quantum-mechanical method PM3 which is a simplified version of Hartree–Fock theory using experimentally derived corrections [44,45]. The method is based on the neglect of diatomic differential overlap (NDDO) integral approximation and implemented in commercially available package HyperChem®. The convergence limit for total electron energy during iterations of the geometry optimization has been set to 0.01 kcal/mol and spin calculations have been performed with the restricted Hartree–Fock method. The geometry optimization algorithm is based on the Polak–Ribiere conjugate gradient method. Properties of the atomistic system such as HOMO and LUMO energies, the corresponding band gap and dipole moments were determined after performing configuration interaction calculations with optimized structure which improves the quality of calculated wavefunctions and state energies.

The mechanical deformation of atomic systems has been simulated by first moving atoms to the position that corresponds to predetermined displacement steps and then performing optimization calculations with displaced atoms being spatially fixed. If targeted displacement of atoms is large then it is divided into smaller fragments and the procedure is repeated for each displacement fragment until a final displacement has been reached.

2.2. Calculation of the second-order deformation gradient

The deformation mapping Φ is introduced relating an initial, reference configuration of the atomic system to the current, deformed configuration, Fig. 1. Positions of the central atom (i) and its neighbours (j, j + 1, ...) in the reference configuration are denoted as $\mathbf{x}^{(i)}$ and $\mathbf{x}^{(j)}$, $\mathbf{x}^{(j+1)}$, ... whereas their counterparts in the deformed configuration are $\mathbf{X}^{(i)}$ and $\mathbf{X}^{(j)}$, $\mathbf{X}^{(j+1)}$, ..., respectively. The inter-atomic distance vectors between atoms (i) and (j) in the reference and deformed configurations are $\mathbf{d}^{(ij)}(d_X, d_Y, d_Z)$ and $\mathbf{D}^{(ij)}(D_X, D_Y, D_Z)$, respectively. The nonlinear approximation of the deformation mapping for each (ij) distance vectors is assumed in the following form:

$$\Phi(\mathbf{d}) = \mathbf{D} \rightarrow \begin{cases} a_1 d_x + a_2 d_y + a_3 d_z + a_4 d_x^2 + a_5 d_y^2 + a_6 d_z^2 + a_7 d_x d_y + a_8 d_x d_z + a_9 d_y d_z = D_X \\ b_1 d_x + b_2 d_y + b_3 d_z + b_4 d_x^2 + b_5 d_y^2 + b_6 d_z^2 + b_7 d_x d_y + b_8 d_x d_z + b_9 d_y d_z = D_Y \\ c_1 d_x + c_2 d_y + c_3 d_z + c_4 d_x^2 + c_5 d_y^2 + c_6 d_z^2 + c_7 d_x d_y + c_8 d_x d_z + c_9 d_y d_z = D_Z \end{cases} \quad (1)$$

The values of 27 polynomial coefficients a_k, b_k, c_k (k = 1, 2 ... 9) can be determined from the information on values of distances between the central atom (i) and its N nearest and near neighbours in the reference (d_x, d_y, d_z) and deformed (D_X, D_Y, D_Z) configurations. The number N of neighbouring atoms is taken larger than nine in order to get a number of equations that exceed the number of unknowns. Then the best approximation of current atomic distances in the sense of least square differences is obtained if $\boldsymbol{C}^T\boldsymbol{C}\boldsymbol{U} = \boldsymbol{C}^T\boldsymbol{D}$, where $\boldsymbol{C}(N \times 9)$ is the matrix of polynomial components (d_x, d_y, d_z) from Eq. (1) for N atoms, $\boldsymbol{U}(9 \times 3)$ is the matrix of nine unknown polynomial coefficients and $\boldsymbol{D}(N \times 3)$ is the matrix of inter-atomic distances (D_X, D_Y, D_Z) for N neighbours. This matrix equation can be solved using the standard Gauss elimination technique providing the deformation mapping Φ in an explicit form. Thus the transformation between the reference and the deformed state of the distance vector from the atom (i) to its neighbour (j) can be written as:

$$\mathbf{D}^{(ij)} = \mathbf{F}\mathbf{d}^{(ij)} + 1/2\ \mathbf{G} : [\mathbf{d}^{(ij)} \otimes \mathbf{d}^{(ij)}] \quad (2)$$

where **F** is the first derivative of the mapping corresponding to the linear deformation gradient and **G** is the second derivative representing the second-order deformation gradient. In a similar way the mapping of atom positions i.e. atomic coordinates can be performed to match an atomic configuration in the deformed state [46]. Quantities **F** and **G** are assigned to every atom in the system the former representing homogeneous deformation and the later characterizing non-homogeneous deformation.

3. Analysis and discussion

To investigate the role of the second-order deformation gradient in the description of locally highly non-homogeneous

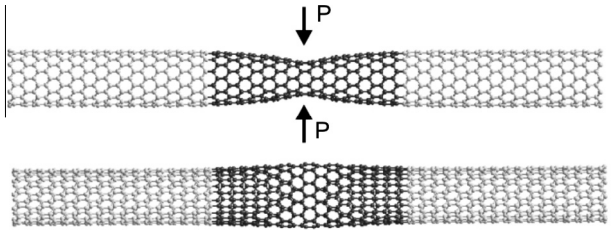

Fig. 2. Locally deformed SWCNT.

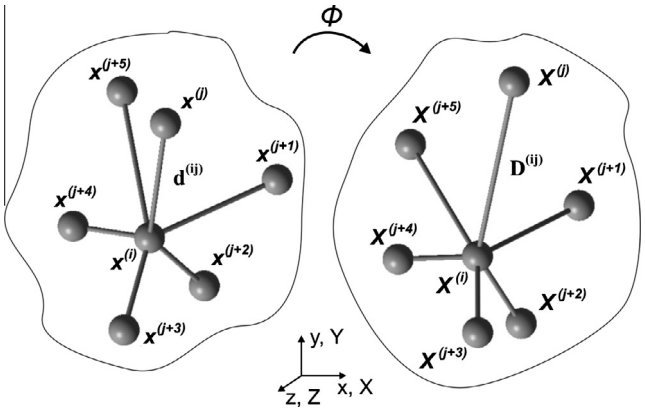

Fig. 1. Deformation mapping from the initial to the current configuration.

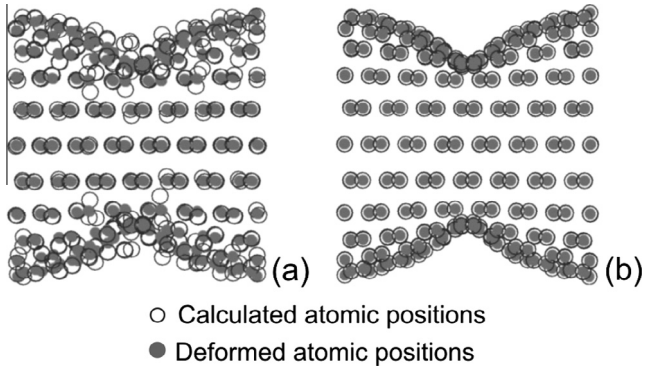

Fig. 3. Comparison of deformed atomic positions from PM3 calculations of the SWCNT with solutions that are based on the modified least square (a) and the second order gradient mappings (b).